11-2011

Controlling the wave focal structure of metallic nanoslit lenses with liquid crystals

S Ishii
Purdue University, sishii@purdue.edu

A V. Kildishev
Purdue University, kildishev@purdue.edu

V M. Shalaev
Purdue University, shalaev@purdue.edu

V P. Drachev
Purdue University, vdrachev@purdue.edu

Ishii, S; Kildishev, A V.; Shalaev, V M.; and Drachev, V P., "Controlling the wave focal structure of metallic nanoslit lenses with liquid crystals" (2011). *Birck and NCN Publications.* Paper 837.
http://dx.doi.org/10.1002/lapl.201110077

Abstract: The focusing properties of gold nanoslit lenses are controlled by changing the refractive index of liquid crystal fillings inside the nanoslits. When the liquid crystals are in the isotropic state, the nanoslit lenses have higher transmission than in the case when the liquid crystals are in the nematic state. Additionally, the lens that focuses TM-polarized light shows a sharper focus in propagation direction when liquid crystal is in isotropic state. Our numerical simulations show good agreement with our experimental results. Having external control over the focusing properties of nanoslit lenses could be beneficial for practical applications.

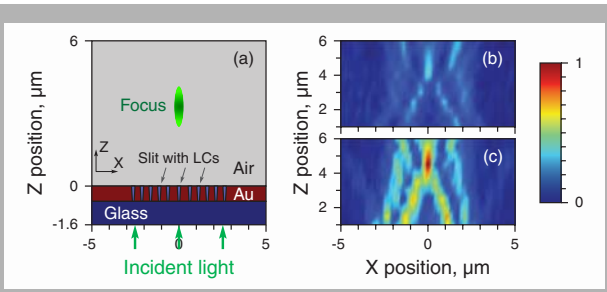

(a) – geometry of the simulation for the TM-lens. The size of the computational domain is $7.6\times10\ \mu m^2$. (b) and (c) – experimental irradiance of the transmitted light for the TM-lens. 2-D plot of the irradiance at room temperature (RT) (b) and at 42°C (HT) (c). The color scale is normalized to the maximum of HT

Controlling the wave focal structure of metallic nanoslit lenses with liquid crystals

S. Ishii, * *A.V. Kildishev, V.M. Shalaev, and V.P. Drachev*

Birck Nanotechnology Center, School of Electrical and Computer Engineering, Purdue University, West Lafayette, IN 47907, USA

Received: 10 June 2011, Revised: 29 June 2011, Accepted: 2 July 2011
Published online: 1 September 2011

Key words: plasmonics; waveguides; nanoslits

1. Introduction

An optical wave transmitted through a slit in a thick metallic film forms a Fresnel diffraction pattern [1]. Since the phase of the wave coming out of a single slit depends on the width of the slit, an array of slits with different widths can be arranged to work as a conventional optical lens [2,3], a beam deflector [4], or a waveguide coupler [5]. The focusing device for TM-polarized light was proposed [3] in 2005, and the device was experimentally demonstrated by L. Verslegers et al. [6] in 2009. In our previous work [7], we conducted a comprehensive study on nanoslit lenses and experimentally showed that arrays of nanoslits can be designed to focus either TM- or TE-polarized light. We have named these devices a TM-lens (for focusing TM-polarized light) and a TE-lens (for focusing TE-polarized light). In the orthogonal incident light polarization, these lenses perform as concave lenses. The lenses demonstrated in [7] are linear, such that the focusing properties cannot be changed as long as the incident beam conditions are fixed.

In optics, liquid crystals (LCs) are known to exhibit large refractive index changes when their orientation or phase changes. Typically, the absolute value of a refractive index change is on the order of 0.1. When LCs are in the nematic phase, the orientation of the LCs can be changed by applying an electric field. Some LC materials have a phase transition temperature in the nematic and isotropic states that are close to room temperature, which makes it easy to control their phases.

When LCs are incorporated into plasmonic structures [8–10], the capability of large refractive index changes offers resonance tunability. When the refractive index of the LC changes, the resonance condition of the plasmonic structure is modified, and this shifts the resonance wavelength of the plasmonic structure. In some recent publications, LCs have been used to tune the resonances of plasmonic nanostructures [11–15] and the metamaterials [16].

* Corresponding author: e-mail: sishii@purdue.edu

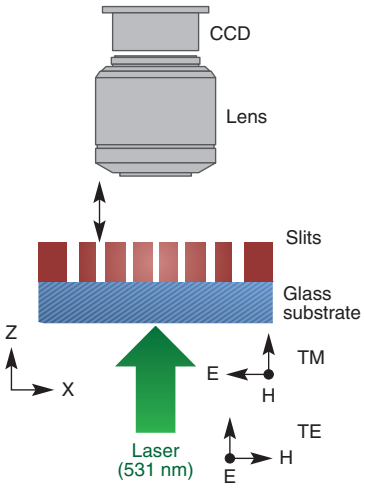

Figure 1 (online color at www.lphys.org) Schematic of the measurement setup. The distance between the lens and the sample was changed to record the irradiance at each Z position

As described in [7], each slit in a nanoslit lens can be considered to be a metal-insulator-metal (MIM) waveguide. Light propagation through a slit is a function of the refractive index of the insulator layer. Thus, it is possible to control the transmission profile of the light coming from the slit by changing the refractive index of the insulator layer. This change could result in either shifting the focal length or changing the intensity and the shape of the transmission profile. In our work, we fill the slits of the nanoslit lenses with LCs to take advantage of their index changing property. We experimentally show that the irradiance as well as the transmission profile change when LCs change their phase from the nematic state to the isotropic state. These LC controllable properties are novel features, which have not been demonstrated in the previous works [6,7].

It is important to note that the purpose of using LCs in our work is to alter the transmission profiles from the nanoslit lenses, while other researchers have used LCs to shift the resonance conditions. The LC used in our study is 5CB (4-cyano-4′-pentylbiphenyl), which has also been used in [16]. The nematic-isotropic phase transition temperature of 5CB is 35°C, which is close to room temperature and thus makes this LC easy to work with experimentally.

2. Experiments and simulations

In our experiments, we first evaporated thick gold films on glass substrates. The film thickness for the TM-lens was 600 nm and the film thickness for the TE-lens was 1000 nm. We then milled the TM-lens and the TE-lens into the films using a focused ion beam (FIB) system. The slits

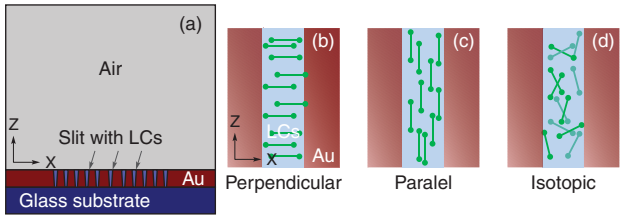

Figure 2 (online color at www.lphys.org) Simulation setting. (a) – geometry of the simulation (TM-lens) and (b)–(d) – orientation of the LCs modeled in the simulations

of each lens were filled with the LC material (5CB, Sigma-Aldrich). The measurement setup is schematically shown in Fig. 1. The samples were illuminated from the substrate side with a linearly polarized continuous wave (CW) laser at 531 nm. The transmission profiles from the lenses were recorded by a CCD camera attached to a conventional optical microscope, allowing us to measure the transmission profiles at varying distances from the lens. The polarization of the incident light for the TM-lens and the TE-lens were TM and TE, respectively. Resolution in the vertical direction is approximately 500 nm due to the resolution of the microscope stage and the depth of focus of the objective lens. All measurements were carried out both at room temperature (22°C, RT) and at 42°C (HT) by heating the microscope stage. More details of the experimental setup could be found in [7].

To verify our experimental results, we have conducted full-wave numerical simulations. The finite element frequency domain (FEFD) method is used for solving 2-D partial differential wave equations for E-field numerically. Thus, a scalar wave equation for E_y is solved in the TE polarization and a vector wave equation for E_x and E_z are solved in the TM polarization case. The 3rd order finite elements are utilized in both polarizations along with generally anisotropic material properties, allowing for the modeling of different phases of the LC component of the device. The computational domain was discretized using an unstructured triangular mesh and then truncated by nonreflecting boundary conditions (scattering boundary condition [17]) applied at all exterior boundaries. The incident light is a monochromatic plane wave forced to propagate from the bottom boundary to the top boundary. The geometrical parameters of the sample were taken from scanning electron microscope (SEM) images. The permittivity of gold is $-12.8 + 1.12i$ at 531 nm from [18], and the refractive index of the LCs was taken from [19]. When simulating for the RT case, we assumed the LC to be in the nematic state and aligned perpendicular to the sidewalls of the gold slits [11,15]. The refractive index tensor was defined as $n = \mathrm{diag}(1.74, 1.55, 1.55)$. When simulating for the HT case, we assumed the LC to be isotropic and defined the refractive index tensor as $n = \mathrm{diag}(1.6, 1.6, 1.6)$. The geometry of the model and the orientations of the LCs are shown in Fig. 2.

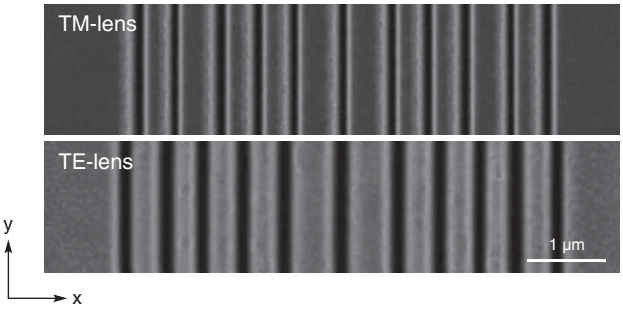

Figure 3 SEM images for the TM-lens (top) and the TE-lens (bottom)

3. Results and discussions

Representative SEM images of the fabricated samples are shown in Fig. 3. Each slit is 22 μm long for both the TM- and TE-lenses. Compared to the wavelength of the illuminating light, the slits are substantially long, and we therefore assume both lenses to be essentially two-dimensional. Both lenses are symmetric with respect to the centerline or center slit. We define the origin of the coordinate at the surface of the lens at center. The X axis is perpendicular to the slits, the Y axis is along the slit and the Z axis is vertical to the sample.

In Fig. 4, we plot the irradiance of the transmitted light from the TM-lens. Fig. 4a is at RT and Fig. 4b is at HT. The color scales for both 2-D plots are identical and normalized to the maximum value recorded at HT. It is clearly seem that the irradiance at HT is higher than the irradiance at RT. The observed change in irradiance can be attributed to the phase change of the LCs inside the slits from the nematic state to the isotropic state.

Fig. 4c and Fig. 4d are the simulation results for TM-lens in the nematic state and the isotropic state, respectively. By comparing Fig. 4c and Fig. 4d, it is obvious that the simulation confirms our experimental results that irradiance is higher in the isotropic state than in the nematic state. The observed changes in irradiance can be qualitatively understood by the following reasoning. Consider TM-polarized light propagating through a MIM waveguide in a plasmonic mode. With the lower permittivity in the dielectric layer, less field penetrate into the metal, thus losses are lower in the metal layer. When the temperature of the LC rises and the LC becomes isotropic, the X component of the permittivity decreases, which results in higher transmission.

The irradiance from the TM-lens at selected z positions obtained from our experiment and the simulation results are plotted in Fig. 4e and Fig. 4f, respectively. The irradiances are normalized to the maximum of each state for both figures. In Fig. 4e, we see that the transmitted light at HT focuses more sharply compared to the transmitted light at RT. At RT it can be assumed that there are local inhomogeneities in the LCs that act to broaden the transmitted profile. At HT the LCs are heated to the isotropic state, and therefore the LCs become more homogeneous. This feature is not captured in the simulated curves since the LCs are simulated as homogeneous media.

In Fig. 5, we show the irradiance plots of the TE-lens. Fig. 5a is at RT and Fig. 5b is at HT. Similar to the TM-lens case, the irradiance at HT is higher than the irradiance at RT. We have also carried out numerical simulations for the TE-lens, the results of which are shown in Fig. 5c and Fig. 5d. In the case of TE-polarized light (electric field in the y direction), the light experiences a refractive index change of 0.05. Fig. 5c is for the nematic state and Fig. 5d is for the isotropic state. From the two 2-D plots, we see that the irradiance in the nematic state is higher than the irradiance in isotropic state, which agrees well with our experimental results. For TE-polarized light propagating through a MIM waveguide in a photonic mode, more field is confined to the dielectric layer when the y component of the permittivity of the dielectric increases, which gives a higher transmission throughput. Thus, heating the LCs to the isotropic state again increases the transmission in this case. The difference in the transmitted irradiance of the TE-lens at the two temperatures is smaller compared to the case of the TM-lens. This is because the refractive index change of the LCs affecting the TE-lens is smaller than the refractive index change of the LCs affecting the TE-lens.

Irradiance from the TE-lens at selected Z positions obtained from our experiments and the simulation results are plotted in Fig. 5e and Fig. 5f, respectively. The irradiances are normalized to the maximum of each state for both figures. From the figures, we do not clearly see the sharpening of transmission profile at HT as we have seen in the TM-lens. We attribute this fact to the smaller effective refractive index change compared to the TM-lens and to experimental noise. In the simulation results, the curves of the two different states almost overlap each other. This is because of the small refractive index difference between the two states.

To gain more quantitative insight, we have plotted the transmitted irradiances along the Z axis in Fig. 6a and Fig. 6b for the TM-lens and the TE-lens, respectively. From the experimental results for the TM-lens, the focal lengths at RT and at HT are 4.0 and 4.5 μm, respectively. At HT, the irradiance at the focus is 2.7 times higher than the irradiance at the focus at RT. From the simulation results, the focal length in the nematic state and the isotropic state are 4.500 and 4.565 μm, respectively. The simulation also shows 2.5 times higher irradiance at the focus for the isotropic state compared to the nematic state. From the experimental results from the TE-lens, the focal lengths at RT and HT are identical at 4.0 μm. The irradiance at focus for the HT case is 1.3 times higher than the irradiance at focus for RT. The simulation shows that the focal lengths in the nematic state and the isotropic are both 4.129 μm, while the irradiance in the isotropic state at focus is 1.2 times higher than the irradiance in the nematic state. Considering the resolution of our measurement setup and the

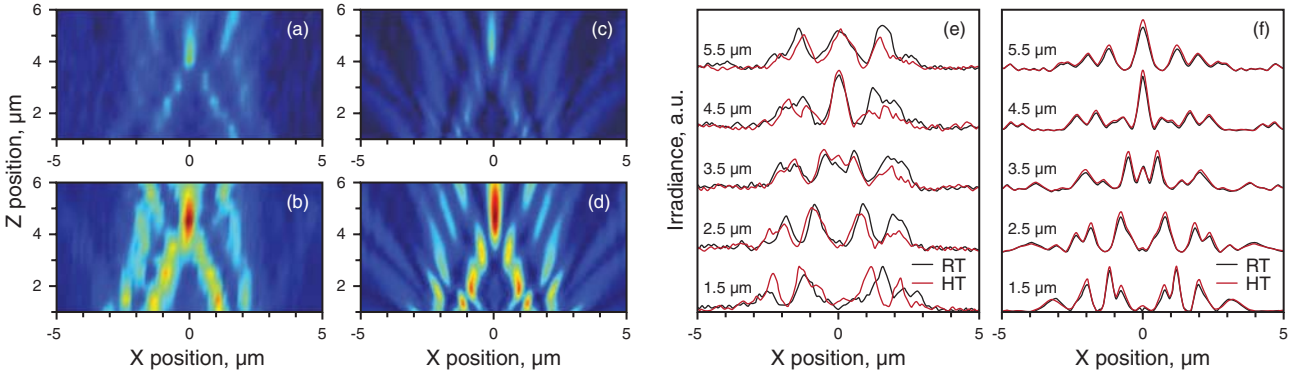

Figure 4 (online color at www.lphys.org) Irradiance of the transmitted light through the TM-lens. (a) and (b) – 2-D plot of the experimentally measured irradiance at RT (a) and at HT (b). The color scale is normalized to the maximum of HT. (c) and (d) – 2-D plot of the numerically calculated irradiance in nematic state (c) and in isotropic state (d). The color scale is normalized to the maximum of the isotropic state. (e) and (f) – irradiance at selected Z positions obtained from the experiment (e) and the simulation (f). In each panel (e) and (f) the curves are normalized to the maxima of the 4.5 μm curves

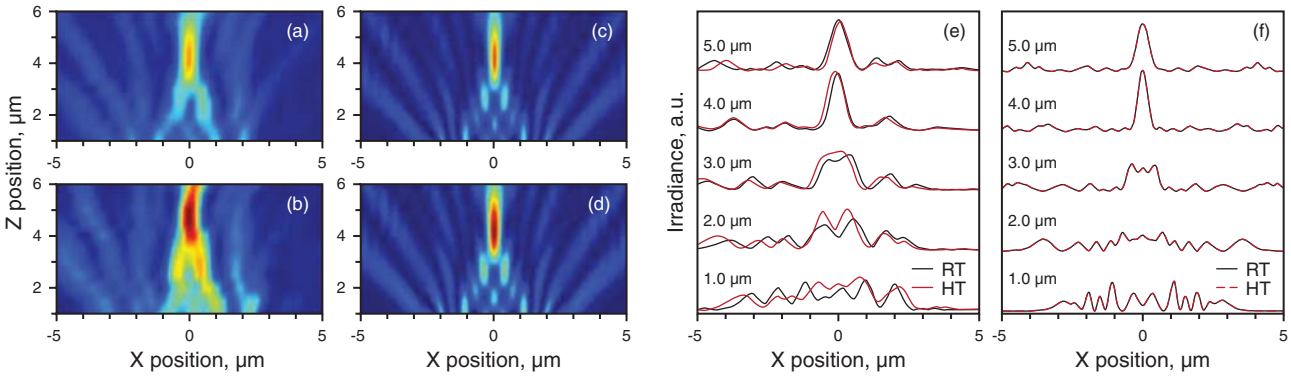

Figure 5 (online color at www.lphys.org) Irradiance of the transmitted light through the TE-lens. (a) and (b) – 2-D plot of the experimentally measured irradiance at RT (a) and at HT (b). The color scale is normalized to the maximum of HT. (c) and (d) – 2-D plot of the numerically calculated irradiance in nematic state (c) and in isotropic state (d). The color scale is normalized to the maximum of the isotropic state. (e) and (f) – irradiance at selected Z positions obtained from experiment (e) and simulation (f). In each panel (e) and (f) the curves are normalized to the maxima of the 4.0 μm curves

nonuniform distribution of the LCs inside the slits, the experimental results and the simulation results are in good agreement.

We also note that P.N. Sanda et al. report that the orientation of 5CB, which is the LCs studied in this paper, is parallel to the gold surface in their studies [20]. Our results confirm an assumption on the orthogonal orientation of LC molecules relative to the wall (called perpendicular in Fig. 2). In order to verify our assumption of the LC orientation, we also simulated a parallel LC orientation inside the slits ($n = \mathrm{diag}(1.55, 1.55, 1.74)$). The results are included in Fig. 6. In the case of the TM-lens, if the parallel orientation of the LCs is assumed for RT, the ratio of the irradiances at focus in the nematic state and the isotropic state is 1.35, which does not correspond to our experimental results. In the case of the TE-lens, the parallel orientation and the perpendicular orientation are equivalent because of the illumination polarization. Therefore, we conclude that the majority of the LCs inside the slits are perpendicularly oriented to the sidewalls of the gold slits in the nematic state.

4. Summary

In summary, we have experimentally shown for the first time that the gold nanoslit lenses whose slits are filled with LCs can have different transmission properties when the phase of the LCs change. For the TM-lens, a sharper focus and a higher irradiance are achieved at HT than at RT. The TE-lens showed smaller changes with respect to the temperature compared to the TM-lens. These observations of the polarization dependence show that the orthogonal orientation is a favorable orientation of the LCs inside the gold slits. The LC controllable focusing properties of

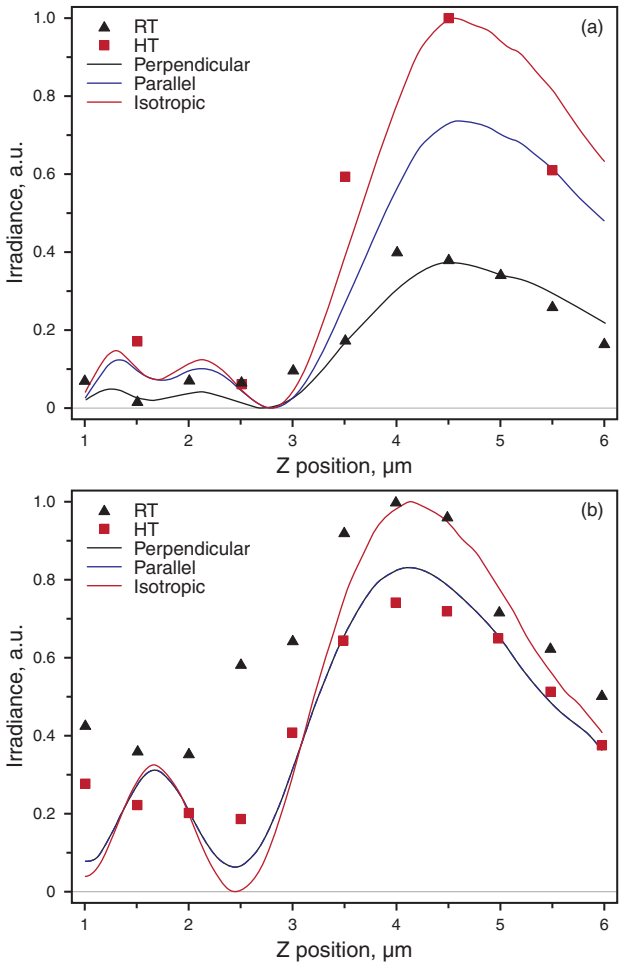

Figure 6 (online color at www.lphys.org) Irradiance along the Z axis for the TM-lens (a) and for the TE-lens (b)

nanoslit lenses could be beneficial for sensing and probing applications in micro/nano optics.

Although the observed changes in transmission in our work are due to the temperature change in refractive index, we do not see significant focal length shifting as shown in [21,22], where nonlinear refractive index was discussed. When the orientation of the LCs filling a nanoslit lens is changed, the refractive index of the LCs changes equally among all the slits and are independent to the width of the slits. On the other hand, when a nonlinear Kerr medium is introduced into the slits, by optically pumping the lens with intense laser, for instance, the changes in refractive index inside the slits depend on the width of the slits. Hence, the phase profile of the transmitted light is altered drastically by changing the optical pumping power, giving larger focal shift.

Acknowledgements This work was supported in part by United States Army Research Office (USARO) Multidisciplinary University Research Initiative program awards 50342-PH-MUR and W911NF-09-1-0539 and by National Science Foundation (NSF) Partnerships for Research and Education in Materials grant DMR 0611430. The authors would like to thank S. Xiao and K.P. Chen for their valuable discussions.

References

[1] M. Born and E. Wolf, Principles of Optics, 3 ed. (Pergamon Press, Oxford, 1965).
[2] Z.J. Sun and H.K. Kim, Appl. Phys. Lett. **85**, 642 (2004).
[3] H.F Shi, C.T. Wang, C.L. Du, X.G. Luo, X.C. Dong, and H.T. Gao, Opt. Express **13**, 6815 (2005).
[4] T. Xu, C.T. Wang, C.L. Du, and X.G. Luo, Opt. Express **16**, 4753.
[5] Y.J. Jung, D. Park, S. Koo, S. Yu, and N. Park, Opt. Express **17**, 18852 (2009).
[6] L. Verslegers, P.B. Catrysse, Z.F. Yu, J.S. White, E.S. Barnard, M.L. Brongersma and S.H. Fan, Nano Lett. **9**, 235 (2009).
[7] S. Ishii, A.V. Kildishev, V.M. Shalaev, K.-P. Chen, and V.P. Drachev, Opt. Lett. **36**, 451 (2011).
[8] V.M. Shalaev, W.S. Cai, U.K. Chettiar, H.-K. Yuan, A.K. Sarychev, V.P. Drachev, and A.V. Kildishev, Opt. Lett. **30**, 3356 (2005).
[9] V.P. Drachev, W. Cai, U. Chettiar, H.-K. Yuan, A.K. Sarychev, A.V. Kildishev, and V.M. Shalaev, Laser Phys. Lett. **3**, 49 (2006).
[10] N.M. Litchinitser and V.M. Shalaev, Laser Phys. Lett. **5**, 411 (2008).
[11] P.A. Kossyrev, A.J. Yin, S.G. Cloutier, D.A. Cardimona, D.H. Huang, P.M. Alsing, and J.M. Xu, Nano Lett. **5**, 1978 (2005).
[12] K.C. Chu, C.Y. Chao, Y.F. Chen, Y.C. Wu, and C.C. Chen, Appl. Phys. Lett. **89**, 103107 (2006).
[13] P.R. Evans, G.A. Wurtz, W.R. Hendren, R. Atkinson, W. Dickson, A.V. Zayats, and R.J. Pollard, Appl. Phys. Lett. **91**, 043101 (2007).
[14] W. Dickson, G.A. Wurtz, P.R. Evans, R.J. Pollard, and A.V. Zayats, Nano Lett. **8**, 281 (2008).
[15] J. Berthelot, A. Bouhelier, C.J. Huang, J. Margueritat, G. Colas-des-Francs, E. Finot, J.-C. Weeber, A. Dereux, S. Kostcheev, H. Ibn El Ahrach, A.-L. Baudrion, J. Plain, R. Bachelot, P. Royer, and G.P. Wiederrecht, Nano Lett. **9**, 3914 (2009).
[16] S.M. Xiao, U.K. Chettiar, A.V. Kildishev, V. Drachev, I.C. Khoo, and V.M. Shalaev, Appl. Phys. Lett. **95**, 033115 (2009).
[17] COMSOL User Manual.
[18] P.B. Johnson and R.W. Christy, Phys. Rev. B **6**, 4370 (1972).
[19] I.-C. Khoo and S.-T. Wu, Optics and Nonlinear Optics of Liquid Crystals, 1 ed. (World Scientific Publishing Co. Pte. Ltd., Singapore, 1993).
[20] P.N. Sanda, D.B. Dove, H.L. Ong, S.A. Jansen, and R. Hoffmann, Phys. Rev. A **39**, 2653 (1989).
[21] C.J. Min, P. Wang, X.J. Jiao, Y. Deng, and H. Ming, Opt. Express **15**, 9541 (2007).
[22] A.V. Kildishev and N.M. Litchinitser, Opt. Commun. **283**, 1628 (2010).